AFWAL-TR-88-4075

FATIGUE CRACK GROWTH CHARACTERISTICS OF ARALL®-1

John J. Ruschau

University of Dayton
Research Institute
300 College Park Avenue
Dayton, Ohio 45469

MAY 1988

Interim Report for Period August 1987 - January 1988

Approved for public release; distribution unlimited.

MATERIALS LABORATORY
AIR FORCE WRIGHT AERONAUTICAL LABORATORIES
AIR FORCE SYSTEMS COMMAND
WRIGHT-PATTERSON AIR FORCE BASE, OH 45433-6533

REPORT DOCUMENTATION PAGE

Form Approved
OMB No. 0704-0188

1a. REPORT SECURITY CLASSIFICATION UNCLASSIFIED	1b. RESTRICTIVE MARKINGS
2a. SECURITY CLASSIFICATION AUTHORITY	3. DISTRIBUTION/AVAILABILITY OF REPORT Approved for public release; distribution unlimited.
2b DECLASSIFICATION/DOWNGRADING SCHEDULE	
4. PERFORMING ORGANIZATION REPORT NUMBER(S) UDR-TR-88-21	5. MONITORING ORGANIZATION REPORT NUMBER(S) AFWAL-TR-88-4075
6a. NAME OF PERFORMING ORGANIZATION University of Dayton Research Institute 6b. OFFICE SYMBOL (If applicable)	7a. NAME OF MONITORING ORGANIZATION Air Force Wright Aeronautical Laboratories Materials Laboratory (AFWAL/MLSE)
6c. ADDRESS (City, State, and ZIP Code) 300 College Park Avenue Dayton, OH 45469	7b. ADDRESS (City, State, and ZIP Code) Wright-Patterson Air Force Base, OH 45433-6533
8a. NAME OF FUNDING/SPONSORING ORGANIZATION Air Force Wright Aeronautical Labs/Materials Lab 8b. OFFICE SYMBOL (If applicable) AFWAL/MLSE	9. PROCUREMENT INSTRUMENT IDENTIFICATION NUMBER F33615-84-C-5130
8c. ADDRESS (City, State, and ZIP Code) Wright-Patterson Air Force Base, OH 45433-6533	10. SOURCE OF FUNDING NUMBERS PROGRAM ELEMENT NO. 62102F; PROJECT NO. 2418; TASK NO 07; WORK UNIT ACCESSION NO. 03

11. TITLE (Include Security Classification)

FATIGUE CRACK GROWTH RATE CHARACTERISTICS OF ARALL®-1

12. PERSONAL AUTHOR(S)

John J. Ruschau

13a. TYPE OF REPORT	13b. TIME COVERED	14. DATE OF REPORT (Year, Month, Day)	15. PAGE COUNT
Interim	FROM 8/87 TO 1/88	May 1988	36

16. SUPPLEMENTARY NOTATION

17. COSATI CODES		
FIELD	GROUP	SUB-GROUP
11	04	

18. SUBJECT TERMS (Continue on reverse if necessary and identify by block number)

ARALL, FALSTAFF, Electrical-Potential, Fatigue Crack Growth, Mini-TWIST

19. ABSTRACT (Continue on reverse if necessary and identify by block number)

Constant amplitude and spectrum fatigue crack growth rate properties were evaluated for ARALL®-1 aluminum laminate. Testing was performed on M(T) specimens under both lab air and high humidity conditions. Crack length monitoring was performed on each aluminum ply utilizing electrical-potential drop techniques to gain a better insight into the fatigue cracking process.

Results indicate an outstanding superiority of ARALL-1 in terms of fatigue crack growth resistance over conventionally produced 7000 series aluminum. Fatigue cracking in each of the aluminum plies was fairly uniform, with no large discrepancies in total crack length or growth rates observed between the various plies. For samples tested under a fighter-type load history, the effect of high humidity was actually beneficial, with fatigue crack growth rates typically one-half of those developed under lab air conditions. Explanations based on increased delamination regions are offered to explain this behavior.

20 DISTRIBUTION/AVAILABILITY OF ABSTRACT	21. ABSTRACT SECURITY CLASSIFICATION
☒ UNCLASSIFIED/UNLIMITED ☐ SAME AS RPT. ☐ DTIC USERS	UNCLASSIFIED
22a. NAME OF RESPONSIBLE INDIVIDUAL M.A. Phillips	22b TELEPHONE (Include Area Code) 513-255-5063
	22c OFFICE SYMBOL AFWAL/MLSE

DD Form 1473, JUN 86 — Previous editions are obsolete

PREFACE

This interim technical report was submitted by the University of Dayton Research Institute, Dayton, Ohio, under Contract F33615-84-C-5130, "Quick Reaction Evaluation of Materials," with the Air Force Wright Aeronautical Laboratories, Wright-Patterson Air Force Base, Ohio. This work was administered by the Systems Support Division, Materials Laboratory, with administrative direction provided by Ms. Mary Ann Phillips, AFWAL/MLSE.

This effort was conducted during the period of August 1987 to January 1988. The author, Mr. John J. Ruschau, was Project Engineer and would like to extend special recognition to Messrs. John H. Eblin and Donald Woleslagle of the University of Dayton for their technical support, and to Mr. Noel Tracy of Universal Technology Corporation for his support in the X-ray inspection efforts.

This report was submitted by the author in May 1988.

TABLE OF CONTENTS

LIST OF ILLUSTRATIONS

SECTION 1
INTRODUCTION

ARALL®, a recently developed aluminum laminate, has become a serious contender for tension-dominated, aluminum sheet applications within the aerospace community. The concept of alternating plies of thin aluminum alloy sheet in combination with layers of fiber reinforced resins (prepregs) was developed at the Delft Technical University[1] and is now being commercialized by ALCOA.[2] Higher tensile strength, improved fatigue and fracture resistance, and lower density, along with good formability and machinability are just some of the reported advantages ARALL has over its all aluminum or all composite counterparts today. However, the majority of reported property improvements have resulted from standardized coupon testing under laboratory-type conditions. In order for ARALL to be properly accepted as a viable sheet replacement, its performance under real life service conditions must be more thoroughly characterized.

The term ARALL is the exclusive property of ALCOA and currently designates a group of four laminated sheet products referred to as ARALL-X, where X is a number between 1 and 4. Each of these ARALL numbers represents a different aluminum sheet material and/or a different stretch during processing. In this effort, the fatigue crack growth rate properties of ARALL-1 are investigated under both simplified laboratory (constant amplitude) and simulated service (spectrum) loading conditions. The loading histories employed for the latter were FALSTAFF, representative of a fighter type aircraft lower wing skin, and Mini-TWIST, an abbreviated transport aircraft load history. Growth rate data obtained are compared to currently used aerospace aluminum sheet products. Under the FALSTAFF spectrum, the effects of a high humidity environment on the fatigue crack growth properties are

---

®ARALL is a registered trademark of the Aluminum Company of America.

also examined. Finally, in an attempt to gain further insight into the fatigue cracking process of this unique material, crack growth monitoring was performed on both surface plies, as well as the center ply, using electrical-potential drop techniques.

SECTION 2
MATERIAL AND SPECIMENS

The test material was manufactured and furnished by the ALCOA Technical Center and identified as ARALL-1. The composition of this sheet material consists of three plies of aluminum alloy 7075-T6 aluminum sheet approximately 0.012 inches thick, in combination with two alternating layers of unidirectional Twaron (Enka Co.) aramid fibers impregnated with an AF-163-2 adhesive manufactured by the 3M Company. A schematic illustrating the ARALL-1 layup is furnished in Figure 1. Prior to layup and cure, the aluminum surfaces were chromic acid anodized and primed. Final product thickness was approximately 0.053 inches, with a density equal to 0.083 lb/cu. in. as compared to 0.10 for aluminum 7075. Following panel layup and cure, ARALL-1 is stretched to a permanent deformation of 0.5% to impart a compressive residual stress in the aluminum sheets.

Middle-crack-tension M(T) specimens were machined to the configuration shown in Figure 2, for widths of 4 and 6 inches. The direction of loading of all samples coincided with the fiber orientation. To accommodate the placement of the electrical-potential leads on the interior ply, a slight modification to the starter notch geometry was required, as illustrated in Figure 3. On one side of the specimen, at the center of the notch, a small semi-circle of material was removed from the surface aluminum sheet, just deep enough to expose the central aluminum ply surface. On this surface, 0.001 inch diameter aluminum potential lead wires were welded, straddling the notch, using a Kulicke and Soffa ultrasonic wire bond welder. A similar procedure of milling a section of a surface ply to expose the central ply was also performed on the ends of these samples to accommodate the attachment of the current input wires to each individual ply.

SECTION 3
PROCEDURES

All fatigue loading was performed on an MTS servo-hydraulic fatigue test machine. Constant amplitude fatigue crack growth rate (fcgr) testing was performed under lab air conditions with a stress ratio of 0.1, and a test frequency of 20 Hz. Crack length measurements were performed using two methods. First, a 10X traveling microscope with digital readout was used to obtain the crack length of each surface ply. This approach was used on all tests and considered the standard in reference to any other surface crack measuring method. Such a procedure required a brief interruption in the cyclic loading to obtain accurate crack length measurements. These halts were typically less than 45 seconds.

The second method, used on approximately half the samples, employed electrical-potential drop (EPD) procedures to monitor cracking in each of the three aluminum plies. A thorough description of the computer-based EPD measurement system is offered in Reference 3. Briefly, a dc current of 10A is passed through the sample, with the three aluminum plies treated as three individual samples, wired in series so that only one current power supply was required. Electrical isolation greater than 10^7 ohms between each aluminum ply (prior to current wire hookup), as well as between the sample and the test machine grips was insured before each test. During fatigue cycling EPD measurements across each crack were performed to obtain a record of voltage drop versus load cycles. Values of crack length were then obtained from the voltage measurements by use of the analytical relationship developed by H.H. Johnson[4] for an infinitely long, center cracked panel, where:

$$a = \frac{1}{C}\left[\frac{\cosh\,(C * Y_o)}{\cosh\left[\frac{V}{V_o} * \cosh^{-1}\left[\frac{\cosh(C*Y_o)}{\cos(\cos(c*a_o))}\right]\right]}\right].$$

where: a = pd determined crack length

a_o = calibration crack length from visual methods

V_o = notch voltage corresponding to a_o

W = specimen width

Y_o = pd lead spacing from crack plane

$C = \pi/W$

V = measured pd voltage.

In the above expression, the final crack length and corresponding final notch voltage were used as the calibration point, a_o and V_o. In most cases a post-test linear correction, based on the initial voltage reading and starter notch, was required to achieve a good correlation between the visual surface readings and the corresponding EPD-determined crack lengths. In general, the EPD crack lengths and visually monitored values varied by less than 0.002 inches.

Constant amplitude fcgr data was derived using the 7-point, incremental polynomial fitting routine as outlined in ASTM Test Method E-647. The average crack length of the three aluminum plies was used to determine growth rate and stress intensity range. Though linear elastic fracture mechanics principles cannot properly be applied to ARALL, due to its non-homogeneous make-up, stress intensity ranges (ΔK) are nonetheless determined in the manner consistent with E647 for comparisons with conventionally produced aluminum under similar fcgr testing conditions.

Fatigue crack growth rate testing was also performed under the FALSTAFF[5] and Mini-TWIST[6] load spectra. Each of these load histories represents a mix of tension/compression loading, with the magnitude of the larger compressive load cycles equal to approximately 25% of the peak tensile stress for each spectrum. A portion of each load history is furnished in Figure 4. Crack length measurements were performed in a manner similar to the constant amplitude tests. Loading frequency was approximately 5 Hz for each spectrum type. Because of the compressive loads occurring in each spectrum, a buckling

restraint was machined from aluminum channel and secured to each sample. A photo of the restraint is shown attached to a sample in Figure 5. Teflon sheet was placed between the sample and restraint to avoid fretting-induced cracking and to eliminate any load transfer through the restraint.

Spectrum fatigue crack growth rate testing was performed in both lab air and a high humidity (>90% R.H.) environment. For high humidity testing, plexiglass panels were secured to the restraining device to form a near airtight chamber on each specimen side. A photograph of this set-up is presented in Figure 6. High humidity air was continuously introduced through each chamber side to insure a relative humidity of greater than 90%.

The secant method was used to reduce the crack length vs. flights test record into the average crack growth rate per flight versus the maximum stress intensity during the growth interval. Since the individual flights of a given spectrum varied considerably throughout one pass of the load spectrum in terms of severity and length and hence crack growth rate, the interval used to establish the growth rate data was one complete spectrum pass. For FALSTAFF, this represented 200 flights, while for Mini-TWIST this was 4,000 flights. By using a complete spectrum pass for the crack growth interval, the effects of load interaction, though observable on a cycle by cycle level, is negated since the crack growth rate is based on a consistent, identical loading "block" and thus comparisons between identically tested samples can be made.

SECTION 4
RESULTS AND DISCUSSION

Constant amplitude fatigue crack growth rate testing on ARALL was conducted in an earlier investigation[3], but results are presented herein with the spectrum data for a more complete picture of the crack growth characteristics of ARALL.

An abbreviated test record of the individual ply's crack length versus cycles for a single, ARALL M(T) sample tested at a maximum cyclic stress of approximately 19 KSI, R=0.1, is presented in Figure 7 and reflects the unusual behavior of this material. Fatigue cracking in each ply started immediately from the machined starter notch at an accelerated rate, then continually slowed down with increasing crack length to a near steady rate (reached approximately after 200 kilocycles). Cracking in each of the aluminum sheets was uniform throughout the crack length range examined, with the central ply lagging the two surface plies by approximately 0.070 inches for the example shown. For other samples tested, the center ply crack length was approximately the average of the two surface cracks. In no instance was the observed differences between the largest and shortest crack length ever greater than 0.1 inches for the constant amplitude and spectrum tests (later described). There was no evidence of any sporadic crack growth (i.e., crack jumping), nor any significant crack growth rate differences between any of the aluminum plies obtained via the pd techniques.

The test record of crack length versus cycles shown in Figure 7 was reduced to obtain the average fatigue crack growth rate versus stress intensity range, the latter based on the average, through-thickness crack, as outlined in ASTM E647. Results are illustrated in Figure 8, along with similar referenced data for 7075-T6 sheet material.[7] As suggested by the 2a-N plot, and contrary to conventionally produced metallic materials, growth rates tend to decrease with successive load cycling, rather than the common increase until fracture. This

phenomenon is believed due to a crack tip bridging effect by the aramid fibers in the wake of the fatigue crack, reducing the effective stress intensity at the crack tip. As the fatigue crack grows, a delamination zone is created in the fiber/adhesive/aluminum interface regions. A photograph of such delamination regions, produced from a reverse image X-ray of a M(T) sample in which a radio-opaque fluid was introduced into the delamination to highlight the zone, is offered in Figure 9, illustrating the size and shape of these regions. This delamination zone has the effect of increasing the "free length" of the low strain-to-failure aramid fibers, enabling them to withstand fracture to a greater extent as the fatigue crack opens since the opening displacement is distributed over a longer fiber length. Researchers[8] have found that for C(T) specimens machined from ARALL-2, a similarly produced laminate with 2024 aluminum sheet, the extent of the unbroken fibers or bridging zone extends between 3 to 5 mm (0.12 to 0.20 inches) behind the fatigue crack tip. For a crack emanating from a machined edge, there are no fibers to bridge the crack and, hence, cracking occurs at a higher rate, until the fatigue crack extends to a degree where the unbroken fibers become effective in restraining crack opening.

It should be re-emphasized that crack growth rate versus stress intensity relationships, as shown in Figure 8, are based on conventional stress intensity solutions and are invalid for ARALL, since a basic premise of LEFM is that the material be homogeneous and isotropic. A more reasonable approach (beyond the scope of this investigation) might be to relate the crack growth rate to an effective stress intensity parameter, K_{eff}, obtained typically from crack tip opening displacement (CTOD) or crack tip opening angle measurements. Nonetheless, the data are presented in the manner shown merely to illustrate that for the specific cyclic loading conditions, the crack growth rate of ARALL-1 decreases with increasing fatigue crack length, to a rate far below that for monolithic aluminums.

The results of lab air spectrum fatigue crack growth rate testing are shown in Figure 10 for a 4-inch wide M(T) sample under the FALSTAFF load history, with the maximum spectrum stress equal to 30 KSI. This stress was selected to yield a sufficient amount of crack growth data in a reasonable time period; additionally, reference data on similar sized 7050-T76 M(T) specimens was available. Results clearly demonstrate the outstanding advantage in crack growth resistance ARALL has over a current 7000 series sheet product under a complex load history. For identical stressing conditions, the ARALL sample withstood over 26,000 flights before failing in the grip region, whereas the similar sized 7050 sample failed at less than 1,625 flights.

The test records for both a 4- and 6-inch wide M(T) sample are presented in Figure 11 for the Mini-TWIST load spectrum, with maximum spectrum stress equal to 40 KSI. Crack growth behavior of the two samples were similar up to specimen failure, with final crack size expectedly longer for the wider 6-inch sample. Following initiation and some rapid crack growth away from the notch, crack extension preceded in a fairly linear manner up to failure. The data from the 4-inch wide sample is plotted again in Figure 12, along with reference data on a similar sized, 7050-T76 M(T) sample subjected to a maximum spectrum stress one-third that of the ARALL-1 sample: 13 KSI versus 40 KSI. Despite the large differences in magnitude of the loading history, the ARALL material withstood four times as many flights prior to failure, with final crack size longer in the ARALL sample than for the 7050 sheet sample.

The fatigue crack growth data just presented for the two load spectra were reduced to the form of the fatigue crack growth rate (inches/flight) versus the maximum stress intensity. Results are illustrated in Figure 13 for the FALSTAFF spectrum and Figure 14 for the Mini-TWIST load history. Also presented in each figure are the data for the 7050. For both load spectra the crack growth rate data (represented by the cross-hatched area in each figure) plot in a cloud well below the 7050 sheet

data, further illustrating the superior performance ARALL has with respect to conventional aluminum. For an identical stress condition, ARALL under FALSTAFF loading was at least an order of magnitude lower in fatigue crack growth rate than for aluminum 7050. Under the Mini-TWIST spectrum, lower growth rates are achieved with ARALL-1 versus aluminum 7050, the latter tested at a fourth of the ARALL spectrum stress intensity ranges. Data developed under Mini-TWIST for the two ARALL specimen widths plot on top of each other, reflecting the similar slopes of the a vs. flights records shown in Figure 11, and hence similar growth rate properties. Growth rates under Mini-TWIST tend to level off to 2-3 micro-inch per flight with increasing crack length, while the FALSTAFF data displayed a slight yet continual rate decrease with increasing crack extension until test termination.

The effects of high humidity on crack growth are displayed in the crack length verses flights record in Figure 15 for the FALSTAFF spectrum. Once again the behavior of ARALL contradicts conventional aluminum behavior: fatigue cracking was slower for the high humidity environment than for the lab air case. The fatigue crack growth rate data obtained from this record is similarly displayed as fatigue crack growth rate verses stress intensity in Figure 16, along with the previous lab air data. Growth rates are typically half that of the lab air data, decreasing slightly with increasing crack length.

Reasons for the greater crack growth resistance under the high humidity conditions are unclear, but the following explanation is offered. Humidity has long been known to affect matrix dominate properties[9] in composites such as fiber-matrix interface degradation. Assuming moisture is able to be absorbed into the epoxy prepreg layers and into the Aramid fibers themselves[10] through the opened fatigue crack and machined starter notch, such a degradation could lead to a larger delamination zone in the wake of the extending fatigue crack. This larger delamination region would result in less fiber breakage across the extending fatigue crack and hence a larger

degree of crack bridging, further reducing the crack tip driving force relative to lab air conditions. If this apparent advantage in fatigue crack growth resistance is a result of an increased delamination region in the laminate, other properties which are normally adversely affected by such regions (e.g. compressive strength) must be carefully re-evaluated under similar environmental conditions to determine property tradeoffs.

SECTION 5
CONCLUSIONS

Based on limited testing, the fatigue crack growth characteristics of ARALL-1 are vastly superior to conventional aluminum sheet products. Under constant amplitude and variable amplitude lab air testing, ARALL displayed at least a ten-fold improvement in terms of growth rate resistance compared to aluminum 7050 sheet material.

The addition of a high humidity environment during fatigue loading under a fighter aircraft type load history led to growth rates even lower than that developed under lab air conditions. This increase is believed to be a result of greater crack bridging by the aramid fibers caused by an increased delamination region in the prepreg layers.

REFERENCES

1. Vogelesang, L.B. and Gumink, J.W., "ARALL, A Material for the Next Generation of Aircraft. A State of the Art," Delft University of Technology, Report LR-400, August 1983.

2. Mueller, L.N., et al., "ARALL (Aramid Aluminum Laminates): Introduction of a New Composite Material," Presented at the AIAA Aerospace Engineering Conference and Show, Los Angeles, CA, February 1985.

3. Ruschau, J.J., "Constant Amplitude FCGR Behavior of ARALL-1," Univ. of Dayton Research Institute, UDR-TM-86-25, October 1986.

4. Johnson, H.H., "Calibrating the Electric Potential Method for Studying Slow Crack Growth," Materials Research and Standards, September 1965.

5. Various authors, "FALSTAFF, Description of a Fighter Aircraft Loading Standard for Fatigue Evaluation," Joint publication of F&W, Switzerland, LBF Germany, NLR, The Netherlands and IABG Germany, March 1976.

6. Lowak, H., DeJonge, J.B., Franz, J. and Schutz, D., "Mini-Twist, A Shortened Version of TWIST," LBF Report TB-146 (1979), NLR MP 79018U.

7. Damage Tolerant Design Handbook, MCIC-HB-01R, Volume 4, December 1983.

8. Ritchie, R.O., et al., "Fatigue Crack Propagation in ARALL® Laminates: Measurement of the Effect of Crack-Tip Shielding From Crack Bridging," Report No. UCB/R/87/A1049, December 1987.

9. Browning, et al., "Moisture Effects in Epoxy Matrix Composites," AFML-TR-77-17, May 1977.

10. Penn, L., "Physicochemical Properties of Kevlar 49 Fiber," Journal of Applied Polymer Science, Vol. 23, 59-73, 1979.

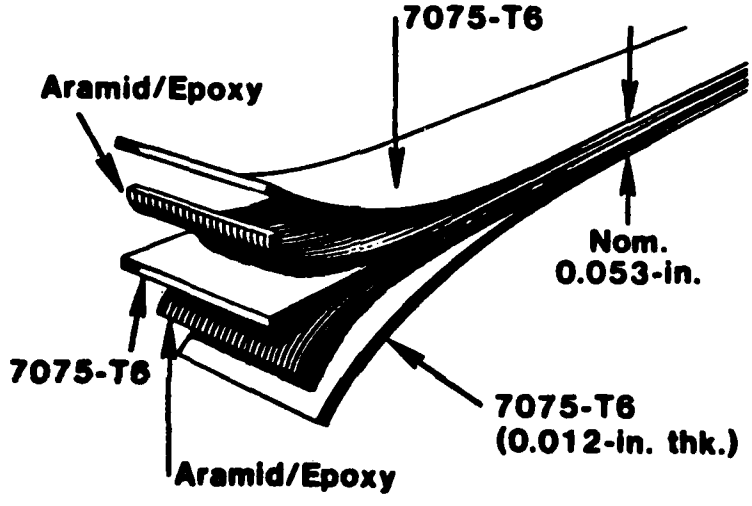

Figure 1. Schematic Lay-up of ARALL-1.

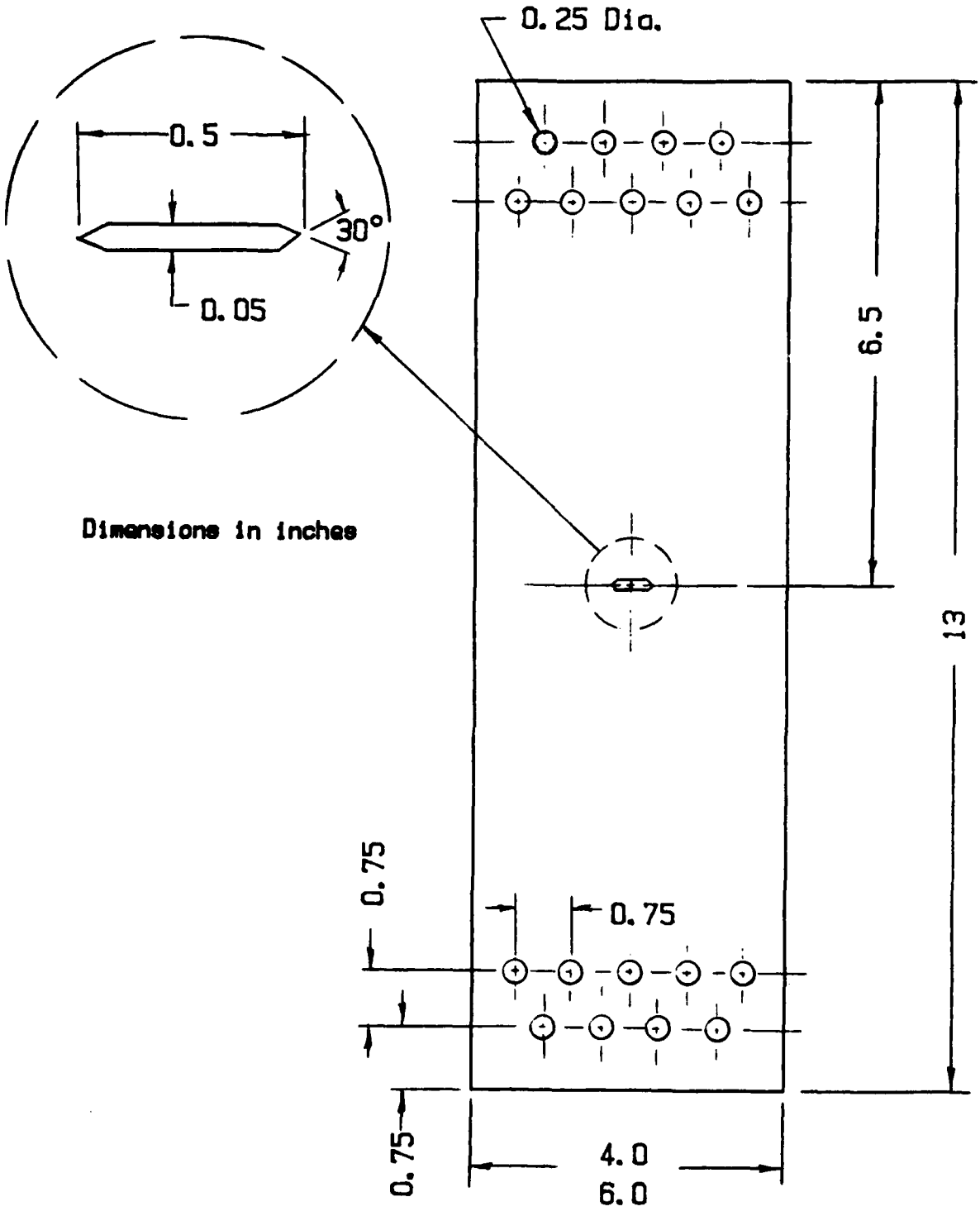

Figure 2. Middle Crack Tension M(T) Specimen Geometry.

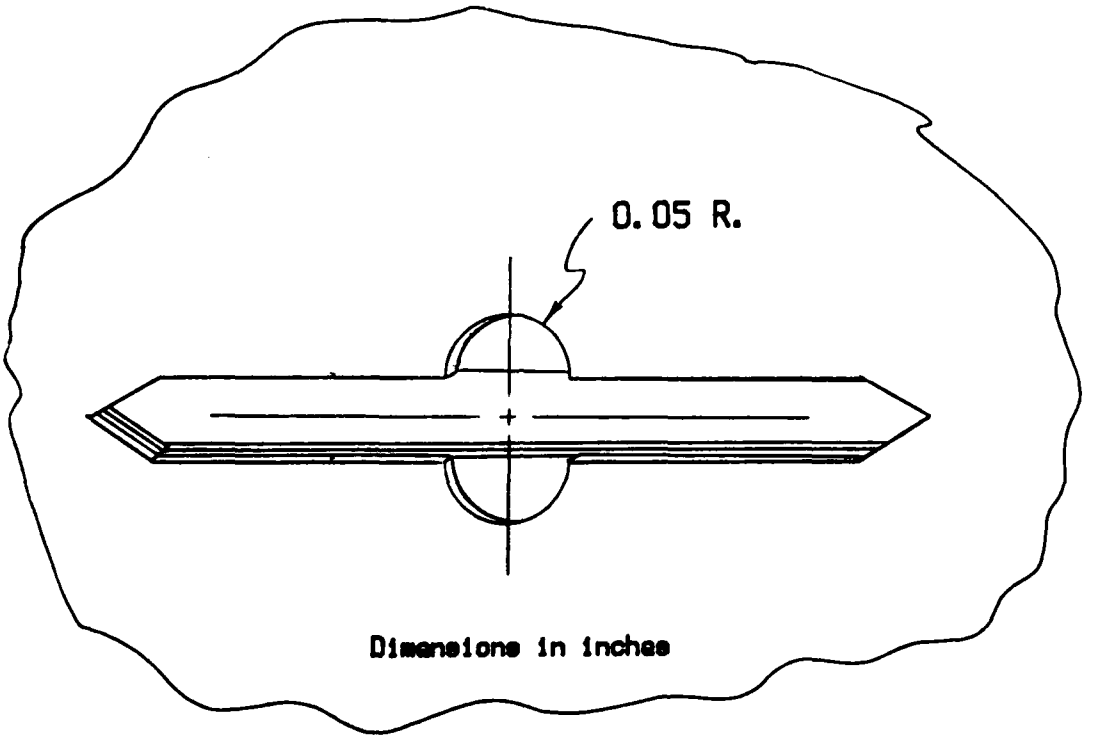

Figure 3. Starter Notch Details.

MINI-TWIST SPECTRUM

FALSTAFF SPECTRUM

Figure 4. Graphical Depiction of Mini-TWIST and FALSTAFF Load Histories.

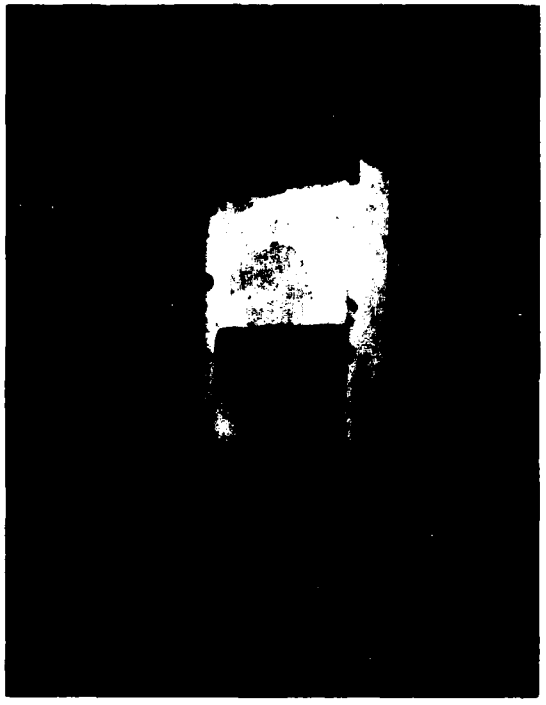

Figure 5. Buckling Restraint for Lab Air Testing.

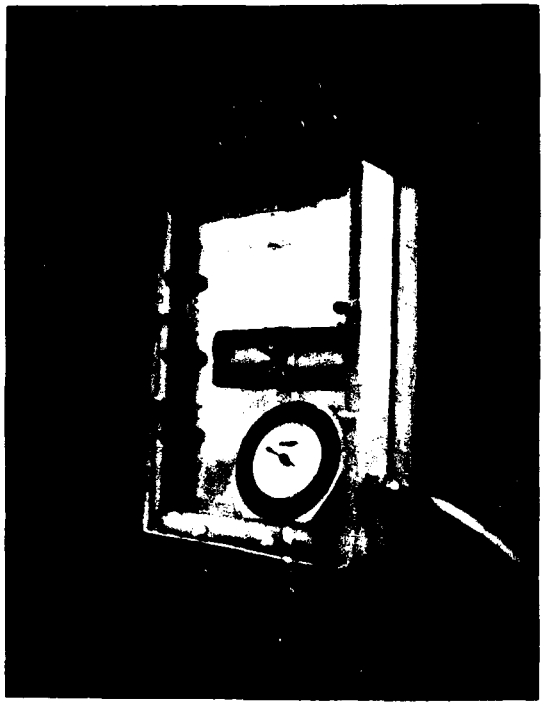

Figure 6. Humidity Chamber with Buckling Restraint.

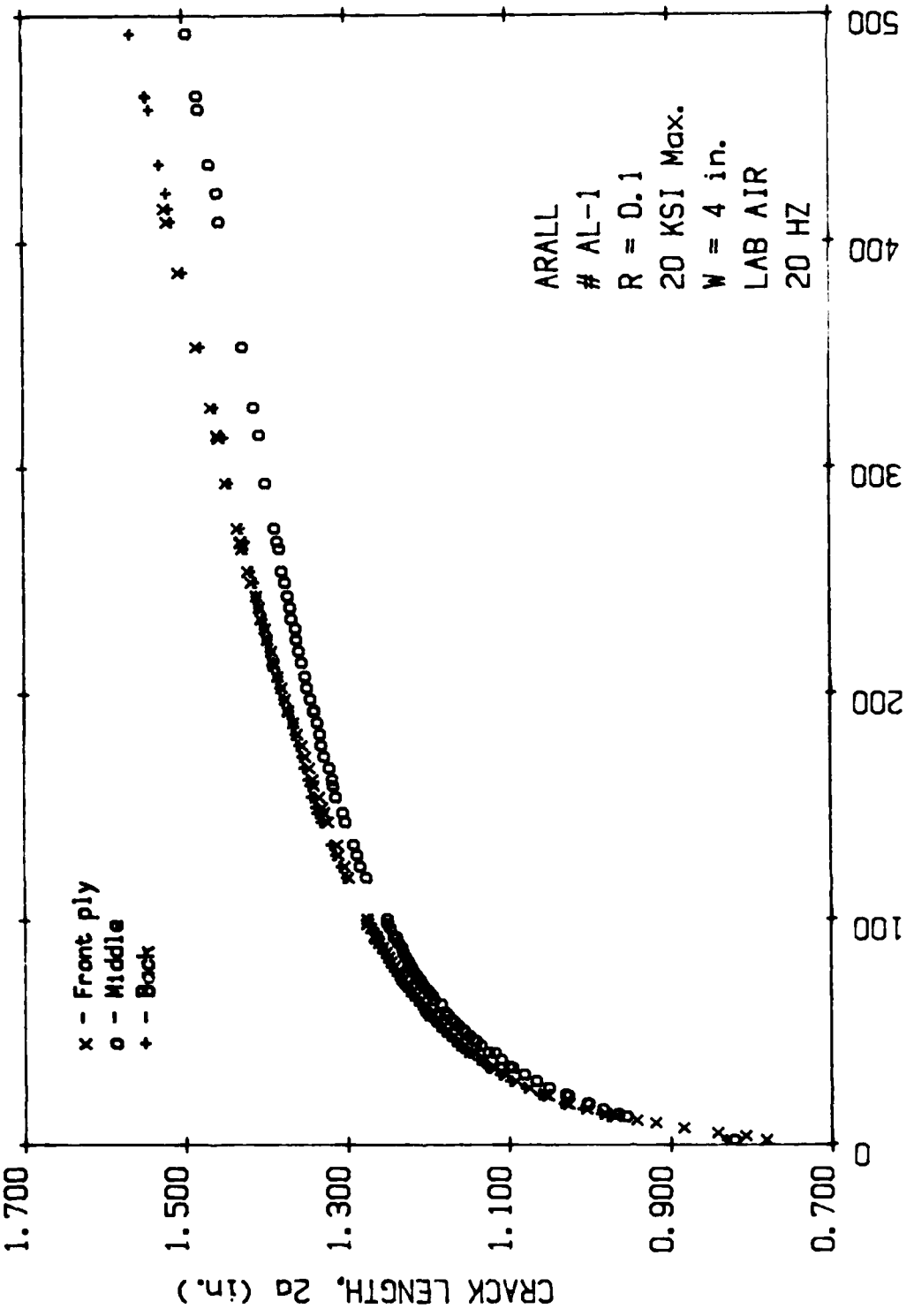

Figure 7. PD-Determined Crack Length vs. Cycles Record for ARALL-1, Constant Amplitude.

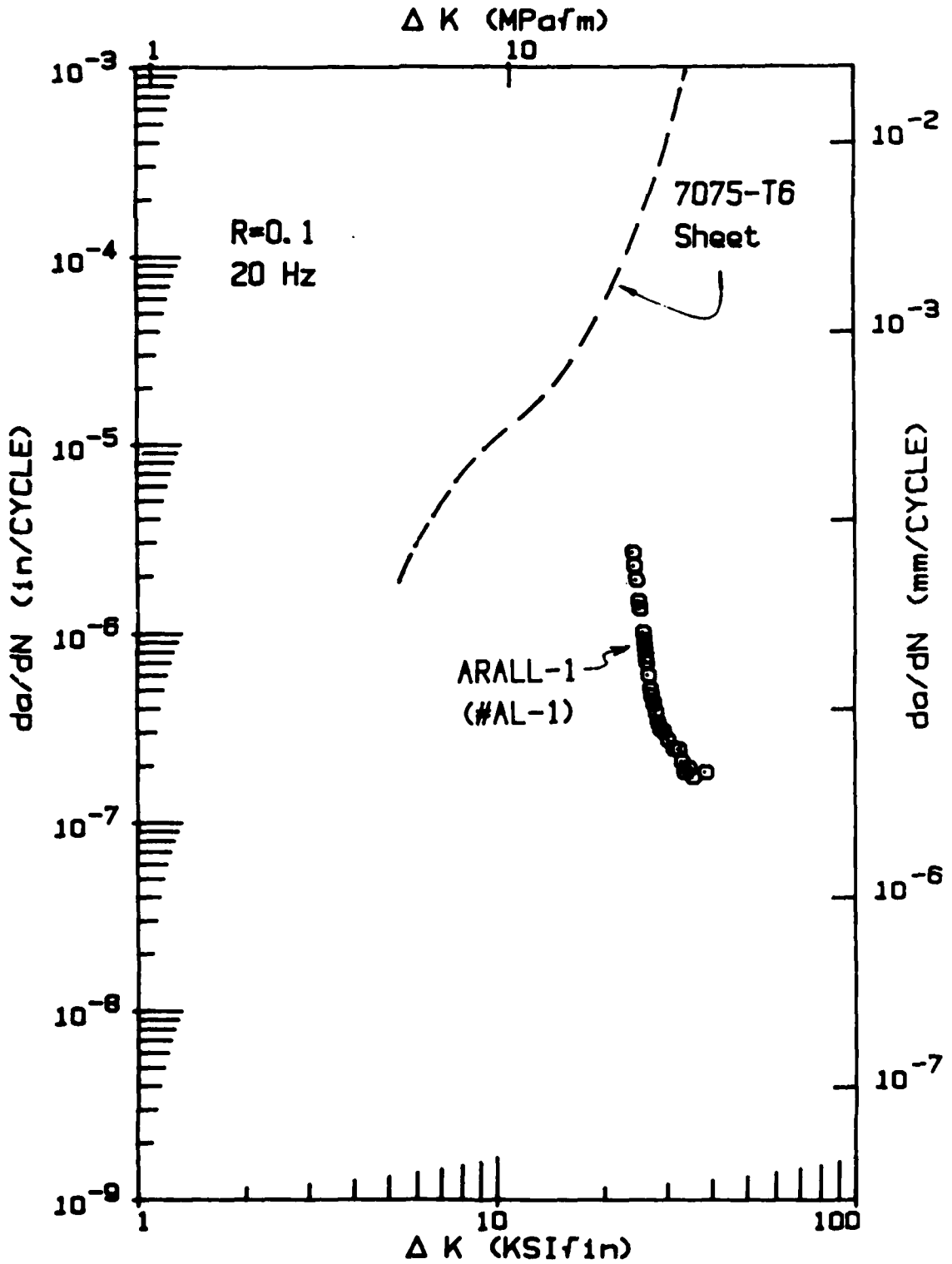

Figure 8. Constant Amplitude FCGR Data for ARALL-1.

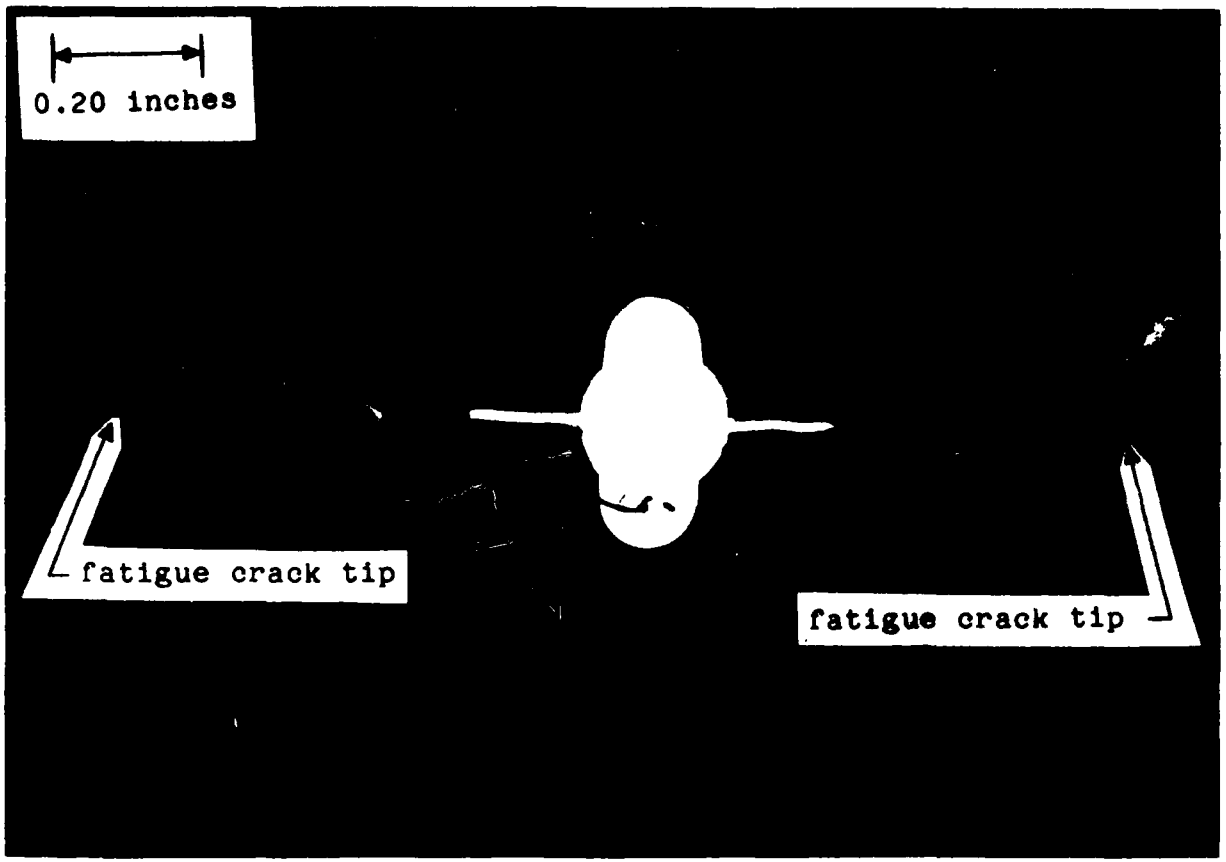

Figure 9. Reverse Image X-Ray of Delamination Zone for ARALL-1 M(T) Specimen.

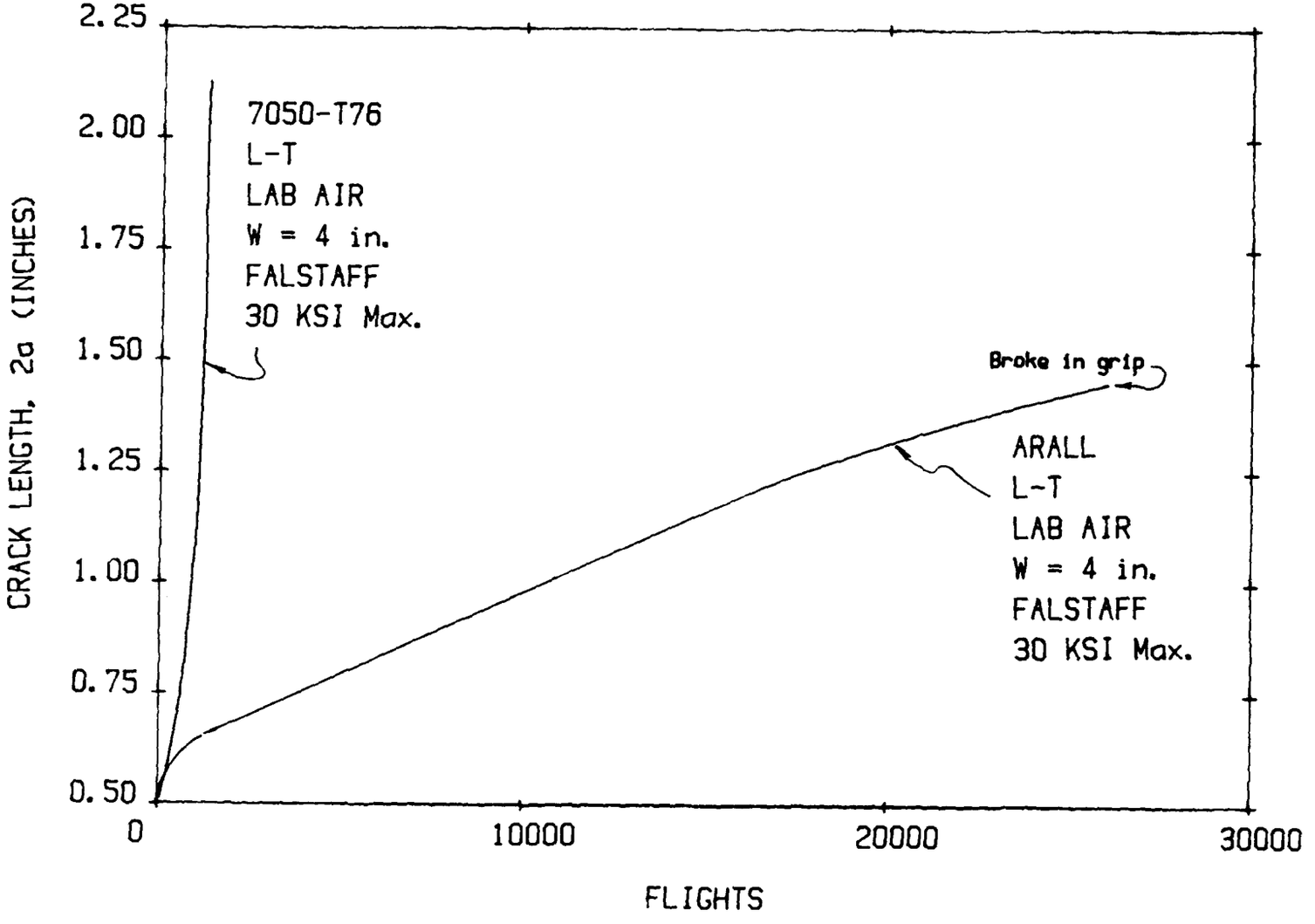

Figure 10. Crack Length vs. Flights Record for ARALL-1 Under FALSTAFF Load History.

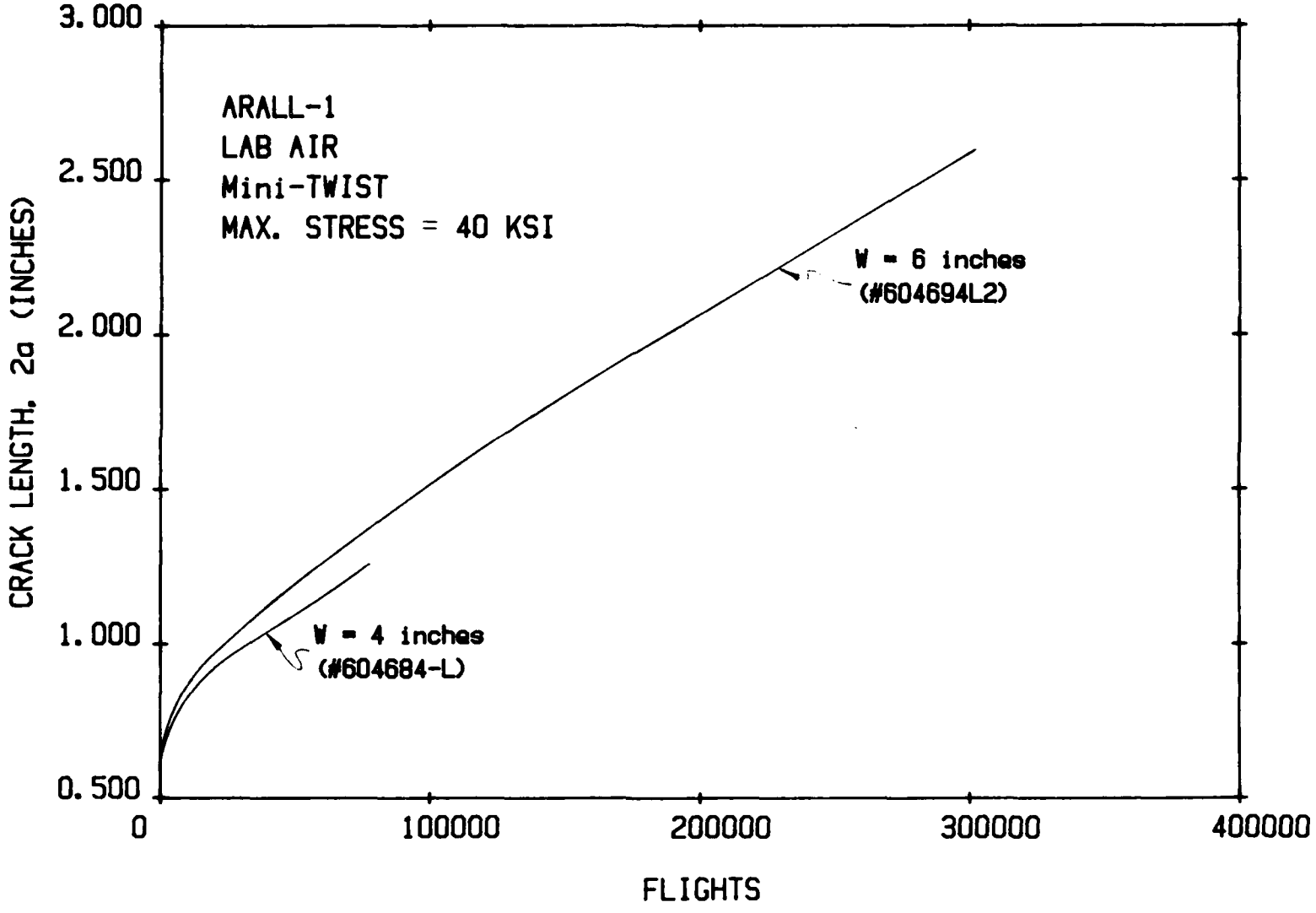

Figure 11. Crack Length vs. Flights Record for ARALL-1 Under Mini-TWIST, W = 4 and 6 inches.

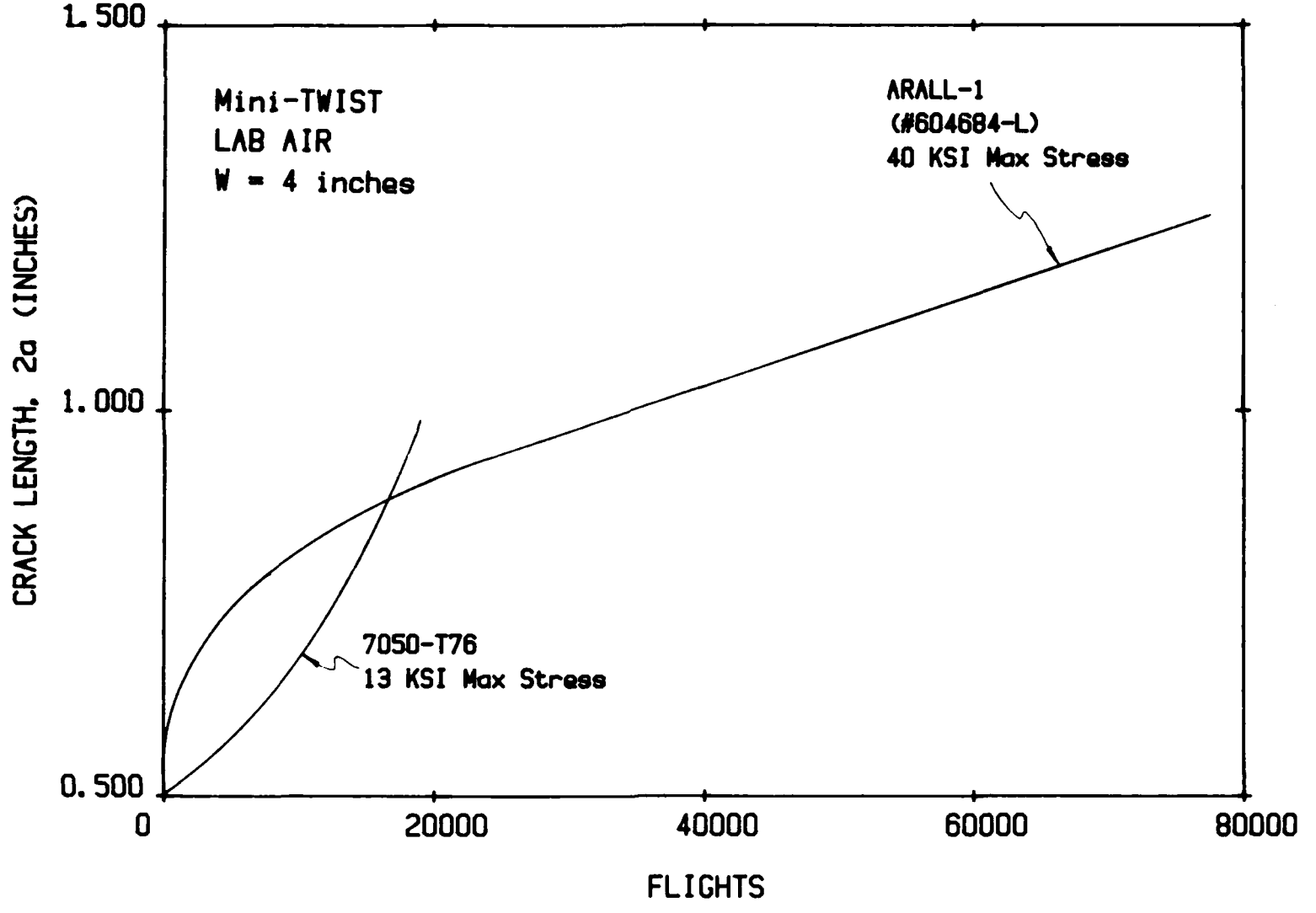

Figure 12. Comparison of Crack Length vs. Flights Records of ARALL-1 and 7050 Under Mini-TWIST.

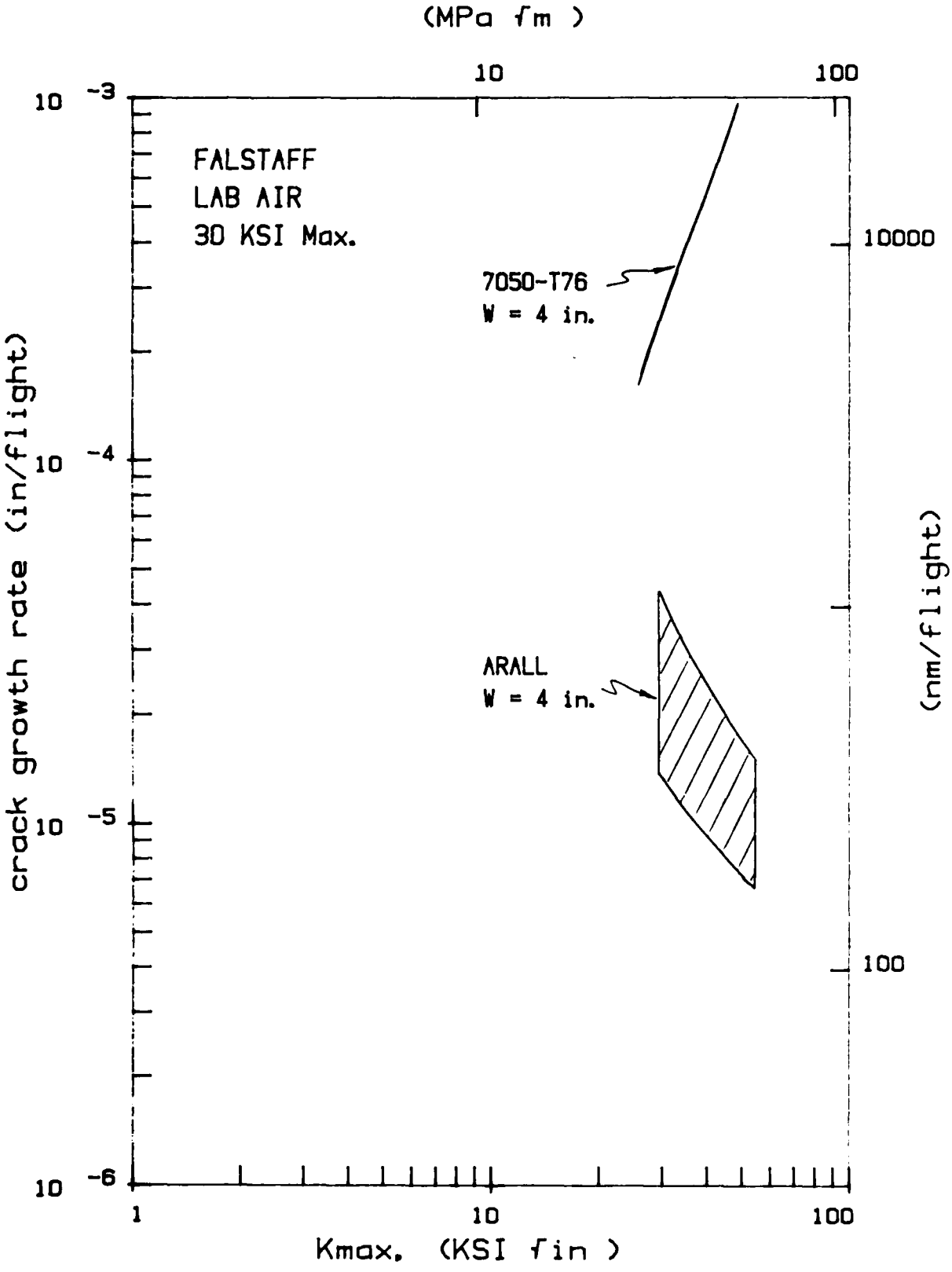

Figure 13. Spectrum FCGR Data for ARALL-1 Under FALSTAFF.

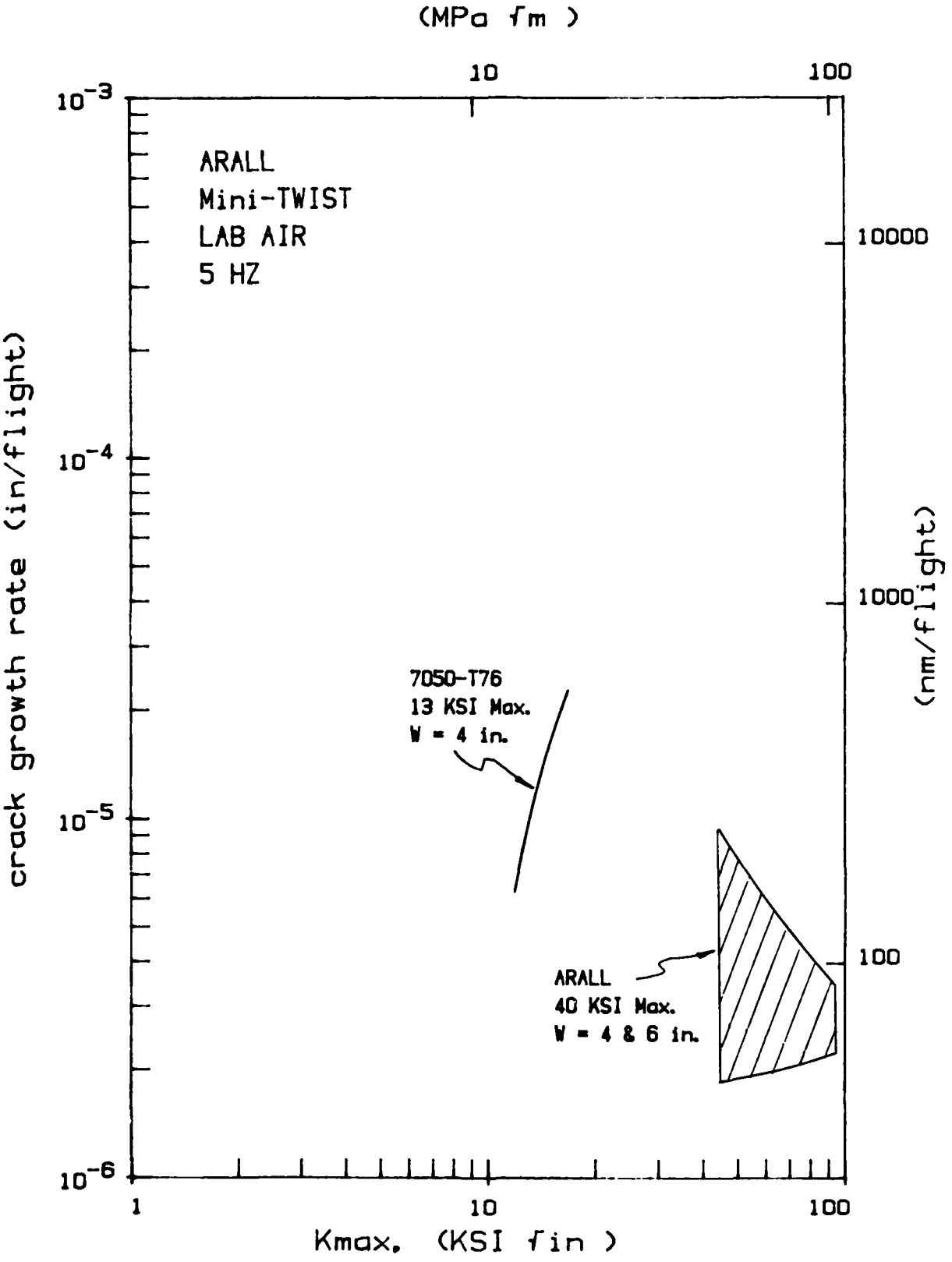

Figure 14. Spectrum FCGR Data for ARALL-1 Under Mini-TWIST.

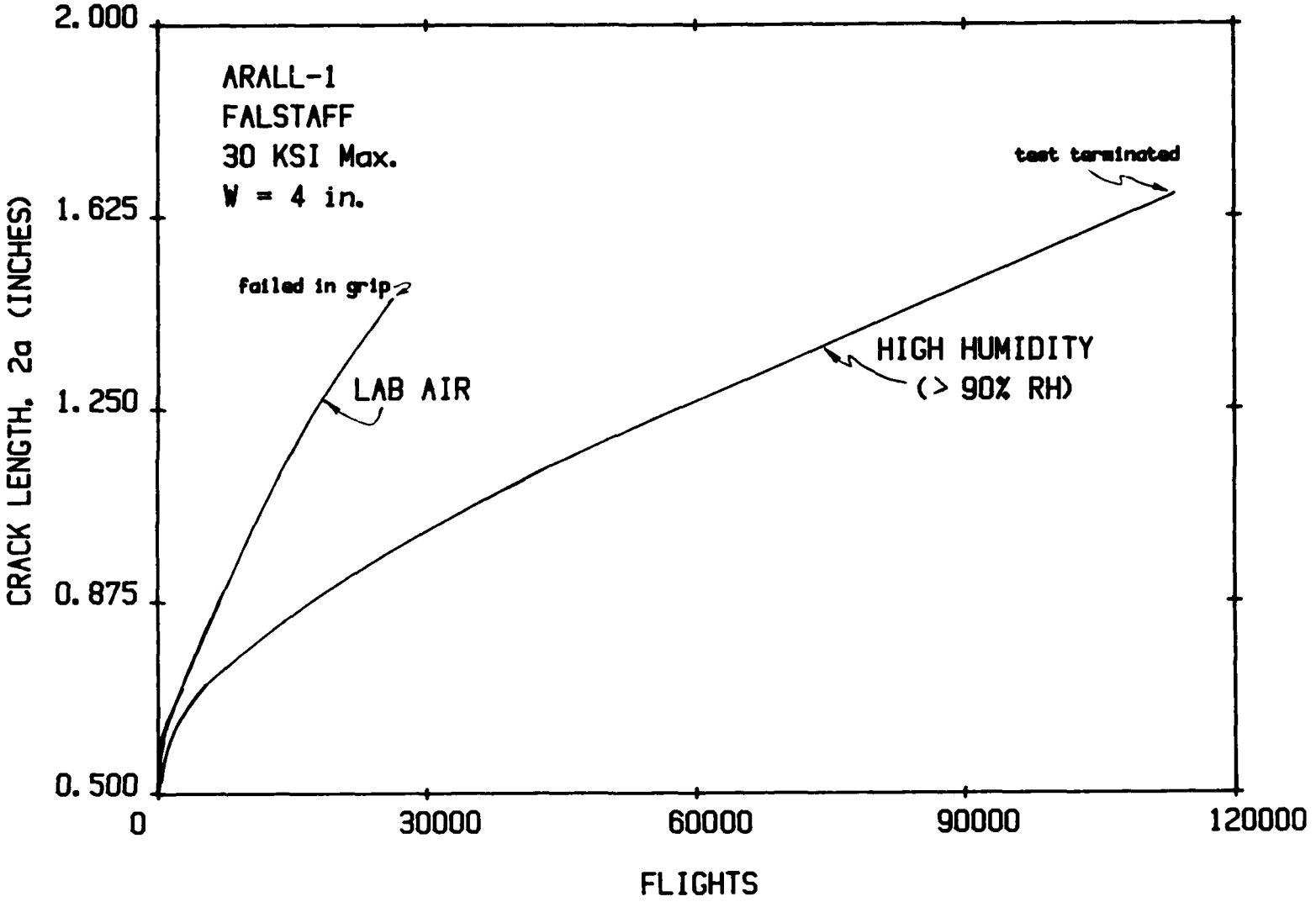

Figure 15. Effect of Humidity on Crack Length vs. Flights Record for ARALL-1 Under FALSTAFF.

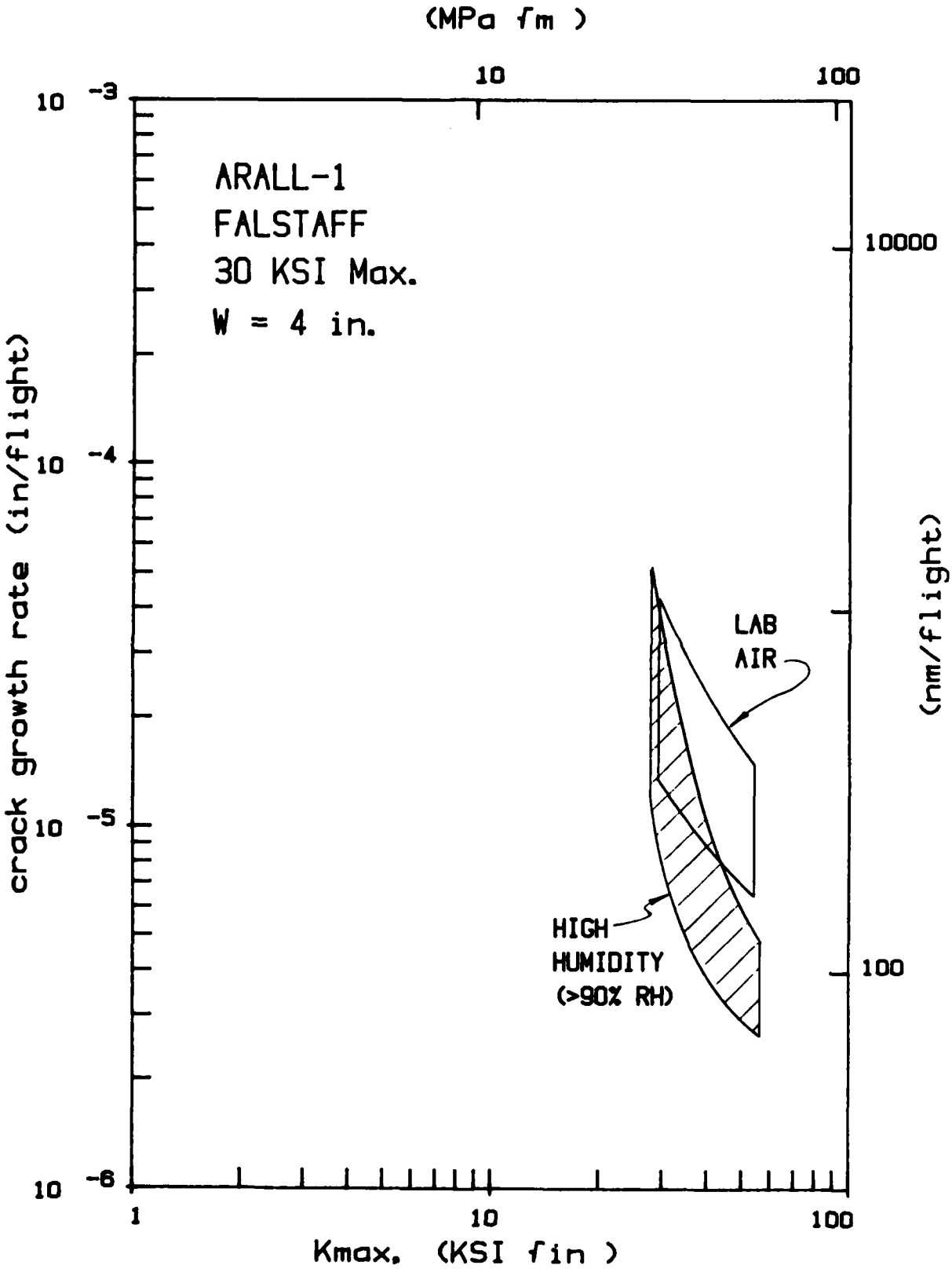

Figure 16. Spectrum FCGR Data for ARALL-1 Under High Humidity Test Environment.